Preparation and Investigation of Thermolysis of L-Aspartic Acid-Intercalated Layered Double Hydroxide

Qi Yuan, Min Wei, David G. Evans, and Xue Duan*

Key Laboratory of Science and Technology of Controllable Chemical Reactions, Ministry of Education, Beijing University of Chemical Technology, Beijing 100029, People's Republic of China

Received: November 6, 2003; In Final Form: June 14, 2004

L-Aspartic acid (L-Asp) has been intercalated into magnesium−aluminum layered double hydroxides by coprecipitation. The structure and composition of the intercalated material have been studied by X-ray diffraction, inductively coupled plasma emission spectroscopy, and elemental analysis. A schematic model of the intercalated structure has been proposed. Furthermore, the thermal decomposition of the hybrid material has been characterized by in situ powder X-ray diffraction, in situ Fourier transform infrared spectroscopy, thermogravimetry, differential thermal analysis, ^{13}C solid-state magic-angle spinning nuclear magnetic resonance, temperature-programmed decomposition, and gas chromatography−mass spectrometry. The thermolysis of L-Asp LDH is quite different from that of the pristine L-Asp studied as a reference sample and is characterized by three steps: the first from room temperature to 150 °C is attributed to the loss of both adsorbed and interlayer water, accompanied by the destruction of the hydrogen bonding network and a decrease in basal spacing; the second step (250∼350 °C) involves the polymerization and deamination of L-Asp ions in the interlayer of LDH and dehydroxylation of the brucite-like layers; the third step in the temperature region of 350∼450 °C corresponds to dehydroxylation of the brucite-like layers as well as further decomposition of interlayer materials.

Introduction

The incorporation of organic guests into layered double hydroxides (LDHs) has received much attention recently because of the potential uses of the resulting inorganic−organic hybrid materials in catalysis,[1−4] optical materials,[5] separation science,[6,7] photochemistry,[8] and electrochemistry.[9] The structure of LDHs may be described in terms of that of brucite ($Mg(OH)_2$) where the cations occupy the centers of octahedra in the close-packed configuration of hydroxyl groups, and the metal octahedra share edges to form two-dimensional infinite sheets. The layers can stack to build a three-dimensional network and are linked by hydrogen bonding between the sheets. In LDHs, a fraction of the divalent cations have been replaced isomorphously with trivalent cations giving positively charged sheets, and there are charge-balancing anions (often carbonate) together with water molecules arranged in interlayers alternating with the brucite-like sheets.[3,10] The water molecules are loosely bound to the hydroxyl groups and can be removed without destroying the structure.[11−13] LDHs may be described by the general formula $[M_{1-x}^{II}M_x^{III}(OH)_2]^{x+}(A^{n-})_{x/n}\cdot mH_2O$, where M^{II} and M^{III} are di- and trivalent metals, respectively, and A^{n-} is the anion. The structure as outlined above was first described by Allmann[14] and Taylor.[15]

Various anionic species have been intercalated into the gallery region of LDHs mainly by coprecipitation or ion exchange (e.g., carboxylic acids,[16] phosphonic acids,[17] cyclodextrin,[18] anionic polymers,[19] drugs,[20] and amino acids[21−23]). However, detailed investigations of the thermolysis of modified LDHs have been rarely reported[24] apart from the case of carbonate-LDHs.

Generally, ex situ X-ray diffraction (XRD) and thermal analysis have been used to investigate the decomposition process of LDHs. Ex situ studies have the disadvantage that mixed oxides derived from LDHs may rehydrate and reconstruct to the original structure at ambient temperature in air.[25] Hou et al.[13] reported the use of relative humidity controlled powder X-ray diffraction (XRD) data that provide greatly increased understanding of the effects of hydration state on the structure and dynamical behavior of interlayer and surface anions and the factors controlling the expansion behavior of this group of minerals. In situ infrared spectroscopy has been employed to provide structural information about the dehydroxylation and decarbonation processes.[25] High-temperature XRD (HT-XRD) has been used as an in situ technique to investigate the decomposition and reconstruction mechanism of $Mg-Al-CO_3$ LDH.[26] In the study, the thermally metastable phases not observed by conventional XRD were characterized by means of the in situ method.

Temperature-programmed reduction (TPR), temperature-programmed desorption (TPD), and temperature-programmed decomposition (TPDE) are powerful techniques used widely in the study of catalysts and surface mediated reactions.[27,28] As most intercalated LDHs release gas during the thermolysis and TPDE reflect that with a characteristic chromatograph signal, the technique may provide considerable insight into the nature of the decomposition process. Furthermore, GC−MS can be used to analyze the composition of the evolved gas. Therefore, we combine TPDE with GC−MS for the first time in the investigation of intercalated LDH species with the aim of providing more evidence about the nature of the decomposition process than is available from thermogravimetry−differential thermal analysis (TG−DTA).

To the best of our knowledge the application of in situ techniques to investigate the thermolysis of biomolecule-intercalated LDHs has not been reported elsewhere. In the

* Corresponding author. Tel: +86-10-64425395. Fax: +86-10-64425385. E-mail: duanx@mail.buct.edu.cn.

10.1021/jp037386v CCC: $27.50
Published on Web 07/23/2004

present work, the mechanism of thermolysis of L-aspartic acid (L-Asp) intercalated LDH has been investigated by in situ FT-IR, in situ HT-XRD, TG-DTA, TPDE and GC−MS. The free amino acid has been studied as a reference sample. This work provides thermal decomposition information for bio-LDH hybrids, which have potential application as novel biomolecule delivery systems that have not been investigated to date.

Experimental Section

Preparation of L-Asp LDH. The matched molar ratio of Mg^{2+}/Al^{3+}/OH-/L-Asp was 2.0/1.0/6.8/1.0. A solution of $Mg(NO_3)_2 \cdot 6H_2O$ and $Al(NO_3)_3 \cdot 9H_2O$ in deionized water was slowly added dropwise to a solution of NaOH and L-Asp with vigorous agitation under a nitrogen atmosphere. The value of the pH at the end of addition was adjusted to 12.5 by further addition of 2.4 mol/L NaOH solution. The reaction mixture was subsequently heated at 100 °C for 6 h, washed with hot deionized water, and dried at 70 °C for 18 h. Elemental analysis gave Mg 23.07%, Al 12.02%, C 7.86%, N 2.48%, and H 4.13%.

Characterization. The in situ powder X-ray diffraction (in situ XRD) measurements were performed on a Rigaku D/MAX2500VB2+/PC diffractometer in the temperature range of 25−700 °C under vacuum conditions, using Cu Kα radiation ($\lambda = 0.154$ nm) at 40 kV, 200 mA, a scanning rate of 5°/min, a step size of 0.02°/s, and a 2θ angle ranging from 2° to 70°. The rate of temperature increase was 10 °C/min with a holding time of 5 min before each measurement.

The in situ Fourier transform infrared (in situ FT-IR) spectra were recorded using a Nicolet 605XB FT-IR spectrometer in the range of 4000−400 cm^{-1} with 4 cm^{-1} resolution under flowing N_2 (65 mL/min) with a heating rate of 5 °C/min in the range 25∼450 °C. The standard KBr disk method (1 mg of sample in 100 mg of KBr) was used.

TG−DTA were measured on a PCT-1A thermal analysis system under normal atmosphere with a heating rate of 5 °C/min. Analysis of metals was performed by ICP emission spectroscopy on a Shimadzu ICPS-7500 instrument using solutions prepared by dissolving the samples in dilute HNO_3. Carbon, hydrogen, and nitrogen analyses were carried out using an Elementarvario elemental analysis instrument. ^{13}C solid-state magic-angle spinning nuclear magnetic resonance (MAS NMR) spectra were run on a Brucker AV300 spectrometer operating at a frequency of 75.467 MHz for ^{13}C at a spinning rate of ∼5000 Hz with a 5 s pulse delay.

TPDE of the samples was carried out using an MRCS-2000 instrument under flowing helium in the range 25−600 °C with a heating rate of 5 °C/min. The decomposition products were analyzed by GC−MS on a Shimadzu GCMS-QP2010 instrument. Helium was used as carrier gas at flow rate of 0.92 mL/min. The injector temperature rise was 250 °C, and the oven temperature was programmed from 30 to 250 °C at a rate of 20 °C/min.

Results and Discussion

Preparation of L-Asp LDH. *Crystal Structure of L-Asp LDH.* The powder XRD pattern of L-Asp LDH is shown in Figure 1. In this case, the reflections can be indexed to a hexagonal lattice with *R*-3m rhombohedral symmetry, commonly used[29,30] for the description of LDH structures. However, as is often the case,[31] several of the (*hkl*) reflections disappear or broaden. The main diffraction peaks of the L-Asp intercalated LDH appear at 7.35° (003), 14.30° (006), and 61.25° (110). In addition, the shoulder at 9−10° 2θ is most likely due to (003) of the Mg−Al−NO_3 LDH phase. Furthermore, the (006) reflection of Mg−Al−NO_3 LDH was observed at 19.70°, which indicates that there is a separate Mg−Al−NO_3 LDH phase mixed in the L-Asp LDH phase. The d_{003} spacing of the L-Asp LDH is 1.20 nm, which is larger than that previously reported by Whilton et al. (1.11 nm).[21] This is possibly because of the different values of pH employed in the reaction, which often gives rise to different basal spacings.[23]

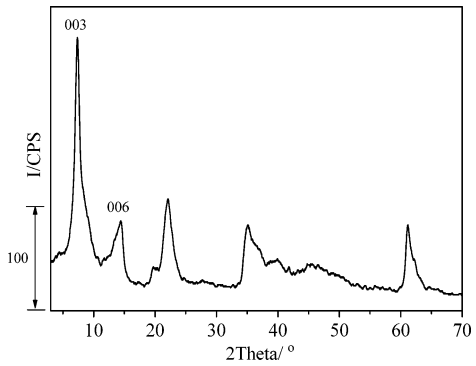

Figure 1. Powder XRD pattern of L-Asp LDH.

LDH materials usually have rhombohedral *R*-3m symmetry. Assuming a 3*R* stacking of the layers and from the positions of the (003), (006), (009), and (110) reflections, the lattice parameters *a* and *c* can be calculated.[32] The value of the lattice parameter *a*, which can be calculated as $a = 2d_{110}$, is a function of the average distance between the metal ions and thus, since Al^{3+} is smaller than Mg^{2+}, gives an indication of the Mg^{2+}/Al^{3+} ratio.[33] The value of *a* for L-Asp LDH is identical to that of Mg−Al−CO_3 LDH, indicating that there is no significant difference in Mg^{2+}/Al^{3+} ratio. The Mg^{2+}/Al^{3+} ratio determined experimentally for L-Asp LDH (2.13) is approximately equal to that in the synthesis mixture (2.00), indicating essentially complete precipitation of metal ions. In contrast, the values of lattice parameter *c* of the two products are quite different. The value of *c* is related to several factors such as the anion size, orientation, and extent of hydration[13] and can be calculated from averaging the positions of the three harmonics, $c = d_{003} + 2d_{006} + 3d_{009}$, although the peak due to 009 reflections is sometimes overlapped with those from other nonbasal planes, which are usually broad because of disorder of the anions and the water molecules in the interlayer space.

Structural Model for L-Asp LDH. Dissociation of L-Asp in water involves three steps arising from the presence of the two carboxyl groups and one amino group in its structure as illustrated in Scheme 1. The values of pK_a are $pK_{a1} = 1.88$ (α-COOH), $pK_{a2} = 3.65$ (R−COOH), $pK_{a3} = 9.60$ (α-NH_3^+), respectively.[34] According to the solution pH and p*Ka* values, the distribution coefficient δ can be calculated. On the basis of the experimental conditions with an aging pH of 12.5, the calculated values of δ are $\delta_1 = 1.77 \times 10^{-5}\%$, $\delta_2 = 0.40 \times 10^{-3}\%$, and $\delta_3 = 99.9\%$; thus, L-Asp exists mainly as the divalent anion -OOCCH(NH_2)CH_2COO- in solution during the aging process. The d_{003} spacing of L-Asp LDH is 1.20 nm. If the thickness of the LDH layer (0.21 nm)[35] and the hydrogen bonding space between the layers and anions (0.27 nm)[35] are subtracted from the basal spacing, the gallery height is calculated to be 0.72 nm, which is approximately equal to the length of the L-Asp anion (0.68 nm, calculated using Chemwindow 6.0). Comparison of the length of the L-Asp anion with the gallery height suggests that L-Asp anions are accommodated vertically in the interlayer region as a monolayer with the two carboxyl groups of individual anions attracted electrostatically to upper and lower hydroxide layers.

SCHEME 1: Dissociation of L-Asp in Water

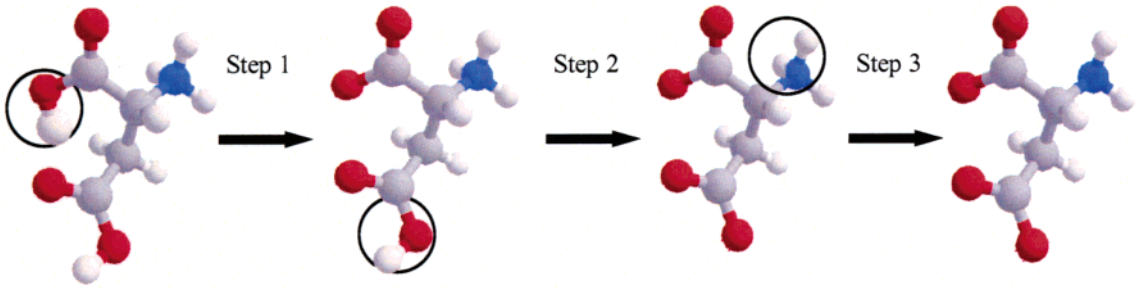

Newman et al.[36] gave a detailed analysis of the arrangement of related amino acid guest species (phenylalanine and tyrosine) in the interlayers using molecular dynamics calculations and concluded that the guests interact with the LDH host layers through a hydrogen-bonding network between them. As L-Asp anion is similar to these guests, therefore, we suggest that the closest contact of the L-Asp anion that is consistent with the existence of hydrogen-bonding interactions to the hydroxide layers is also made through the oxygen atoms of the carboxyl groups. On the basis of the above discussion, a schematic representation of the probable arrangement for the L-Asp LDH is shown in Figure 2. This model will be further discussed in the next section concerning in situ XRD and in situ FT-IR measurements.

Investigation of Thermolysis. *Thermolysis of* L-*Asp.* Thermolysis of L-Asp was studied as a reference sample to allow comparison with L-Asp LDH. The TG and DTA curves of L-Asp are shown in Figure 3 (a1 and a2, respectively). A sharp weight loss in the temperature range of 205−275 °C is due to the polymerization of L-Asp, with two corresponding endothermic peaks in the DTA curve. This is related to the fact that the polymerization of L-Asp involves two steps with one water molecule lost in each,[21] as shown in Scheme 2. The second weight loss between 350 and 420 °C may be attributed to the decomposition and combustion of L-Asp.

As shown in Figure 4a, the TPDE profile displays one main decomposition peak in the temperature range of 340∼380 °C with the maximum at 365 °C, which is attributed to the decomposition of the polymeric mass as H_2O, NH_3, C_2H_4, and CO were all detected in the evolved gas. Furthermore, the weak peak starting at 220 °C is due to water molecules released by the polymerization of L-Asp, since H_2O was detected by GC−MS.

To investigate the polycondensation of L-Asp in more detail, the L-Asp was heated as reported in the literature[21] and was characterized by ^{13}C MAS NMR. Figure 5a,b shows the ^{13}C MAS NMR spectra for L-Asp and L-Asp after heat treatment at 220 °C for 24 h, respectively. For L-Asp, four signals corresponding to carbon atoms with different chemical environments are observed at 175.8 ppm (COOH), 174.7 ppm (COOH), 53.4 ppm (CHN), and 37.5 ppm (CH_2). After heat treatment, the two COOH resonances disappear and a new resonance at 173.9 ppm is observed, which can be attributed to the overlapping imide resonances of CH−C(═O)−N and CH_2−C(═O)−N. The other principal resonances move to lower frequency and are observed at 48.4 ppm (CHN) and 33.5 ppm (CH_2).

Infrared spectra recorded at room temperature, as well as during the decomposition of L-Asp in the temperature range of 25∼450 °C are shown in Figure 6. In the room temperature spectrum, the broad band at 3420 cm^{-1} and the shoulder at 1652 cm^{-1} are due to adsorbed water molecules. The strong absorption at 3017 cm^{-1} along with four weak absorptions in the range of 3050−2400 cm^{-1} can be assigned to N−H stretching and bending vibrations. The absorptions at 1690, 1606, 1516, and 1420 cm^{-1} are assigned to the asymmetric and symmetric COOH stretching vibrations and C═O twisting vibrations. The C−N and C−C stretching modes are observed at 1304 and 1250 cm^{-1}, respectively.[21] Other absorptions in the region 890−550 cm^{-1} arise from the in-plane bending and out-of-plane deformation of C−H or stretching vibrations of CH_2.[37]

As can be observed from Figure 6, no significant changes in the absorption bands of L-Asp are observed on increasing the temperature from 25 to 200 °C apart from the slight decrease in the intensity of the bands. However, there is an obvious change at 250 °C, consistent with the TG−DTA data, due to thermal polycondensation of L-Asp (Scheme 2). The absorption at 1719 cm^{-1} is attributed to the C═O vibration in succinimide, and the band at 1391 cm^{-1} is due to the C−O bending vibration. Furthermore, as the polycondensation reaction is not complete, the two bands at 1209 and 1165 cm^{-1} assigned to the vibrations of C−N in (C═O)−NH and (C═O)−NR−(C═O) are still present at 250 °C but amalgamate to one band at 1175 cm^{-1} when the temperature increases to 300 °C. The bands become weaker with increasing temperature from 300 to 450 °C and are rather weak at 450 °C, consistent with the complete decomposition of polysuccinimide as indicated by TPDE and GC−MS.

Thermolysis of L-*Asp LDH.* The in situ high-temperature powder X-ray diffraction patterns of the intercalation product L-Asp LDH in the temperature range of 20−700 °C are shown in Figure 7.

It can be observed in Figure 7 that the (003) and (006) diffraction peaks of L-Asp LDH move to higher angle 2θ with increasing temperature. The value of d_{003} decreases from 1.20 nm at 20 °C to 0.89 nm at 150 °C, which is related to the destruction of the hydrogen-bonding network as a result of deintercalation of interlayer water molecules. It has been proposed that the layered structure is primarily maintained by hydrogen bonding between interlayer water and guest anions as well as between interlayer species and OH of the metal hydroxide layer.[38,39] The results of this study are consistent with this suggestion, providing further evidence in support of the schematic model for L-Asp LDH proposed in Figure 2. It should be noted that the (003) and (006) diffraction peaks broaden remarkably at 50 °C, which possibly corresponds to an unstable intermediate resulting from the disorder in the arrangement of guests upon the loss of interlayer water. There is no obvious change from 150 to 250 °C, while the intensity of all the reflections decreases between 250 and 400 °C, and all the peaks associated with the LDH disappear at 450 °C. This is related to the decomposition of intercalated L-Asp and dehydroxylation of LDH layers, which will be further discussed below.

The layer structure collapses completely at 450 °C with the first appearance of reflections from a cubic MgO phase at about

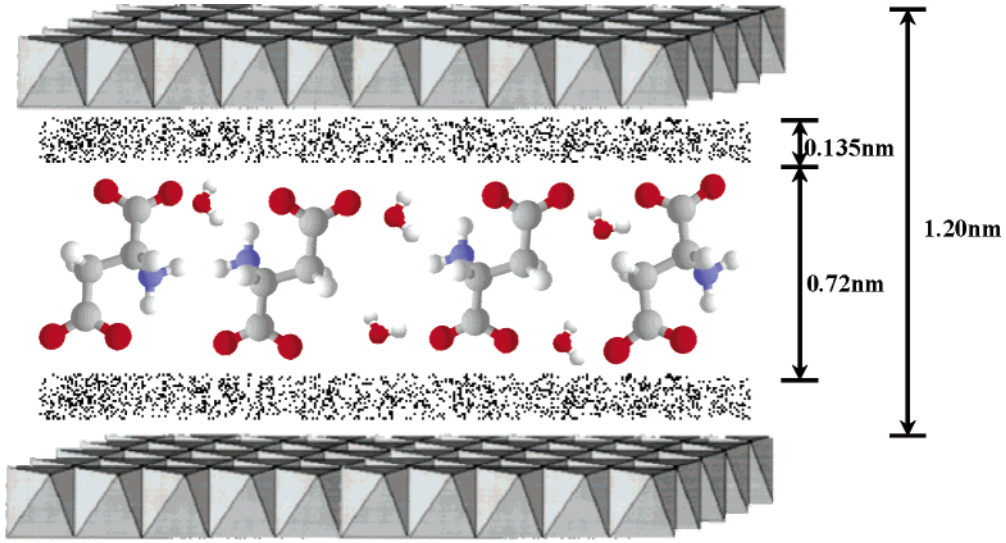

Figure 2. Schematic representation of the possible arrangement for L-Asp LDH.

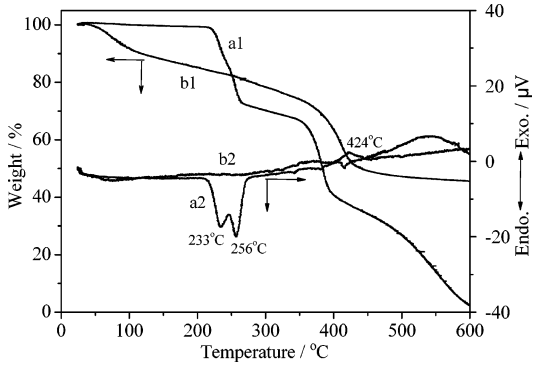

Figure 3. TG and DTA curves for L-Asp (a1, a2) and L-Asp LDH (b1, b2).

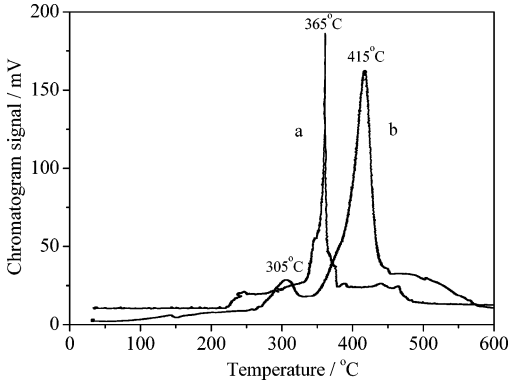

Figure 4. TPDE profiles of (a) L-Asp and (b) L-Asp LDH.

SCHEME 2: Thermal Polycondensation of L-Asp

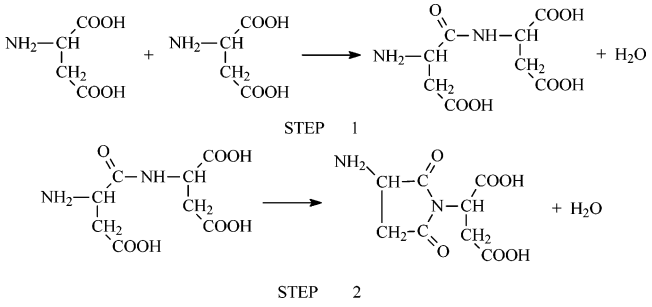

SCHEME 3: Decomposition Reaction of Intercalated L-Asp Anions during Heating

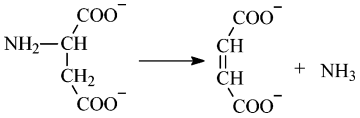

34.6°, 42.8°, and 62.5°. Crystallization of MgO occurs at 450 °C, over 50 °C higher than that usually observed for the calcination of Mg−Al−CO_3 LDH.[12,26,40] Thus, the L-Asp ions probably enhance the thermal stability of the host matrix compared with carbonate. The diffraction peaks of MgO become stronger with increasing temperature from 450 to 700 °C.

The TPDE profile of the L-Asp LDH (Figure 4b) displays three decomposition peaks at 100−150, 250−320, and 350−450 °C. The first weak peak can be ascribed to the loss of interlayer water molecules on the basis of the H_2O detected by GC−MS. The second peak observed at 250−320 °C can be attributed to the decomposition of L-Asp ions and dehydroxylation of the brucite-like layers, because NH_3 and H_2O were detected by GC−MS. The result indicates that initial decomposition of L-Asp ions follows the reaction shown in Scheme 3. In the third temperature range of 350−450 °C, H_2O, C_2H_4, and CO_2 were observed, suggesting that this process corresponds to the further decomposition of guest species as well as the dehydroxylation of the layers.

The TG and DTA curves of the L-Asp LDH are shown in Figure 3 (b1 and b2, respectively). The thermal decomposition of the L-Asp LDH is characterized by three weight loss steps: the first one from room temperature to 150 °C corresponds to the removal of surface adsorbed water (below about 100 °C) and interlayer water molecules resulting in the decrease in interlayer spacing observed in Figure 7; the second one (250∼350 °C), involving a gradual weight loss, is a result of the decomposition of L-Asp ions and dehydroxylation of the brucite-like layers; the third one with a sharp weight loss in the temperature region of 350−450 °C with a corresponding exothermic maximum at 424 °C in the DTA is due to dehydroxylation of the brucite-like layers as well as combustion of the decomposed materials.

The in situ FT-IR spectra of L-Asp LDH are shown in Figure 8. At room temperature, the broad absorption band at 3450 cm^{-1} is attributed to the stretching vibrations of the hydroxyl group in the LDH layers and interlayer water molecules, which occur at lower frequency compared with the O−H vibration in free

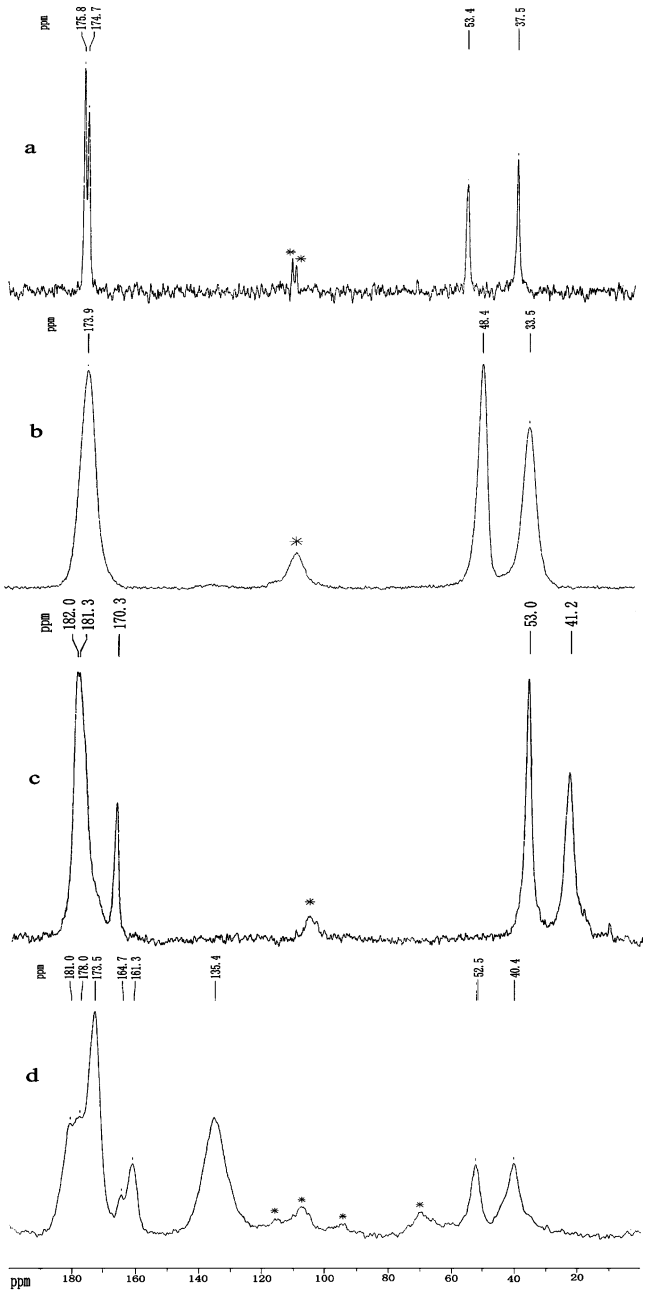

Figure 5. ^{13}C MAS NMR spectra for (a) L-Asp, (b) L-Asp after heat treatment at 220 °C for 24 h, (c) L-Asp LDH, and (d) L-Asp LDH after heat treatment at 220 °C for 24 h. Asterisks indicate spinning sidebands.

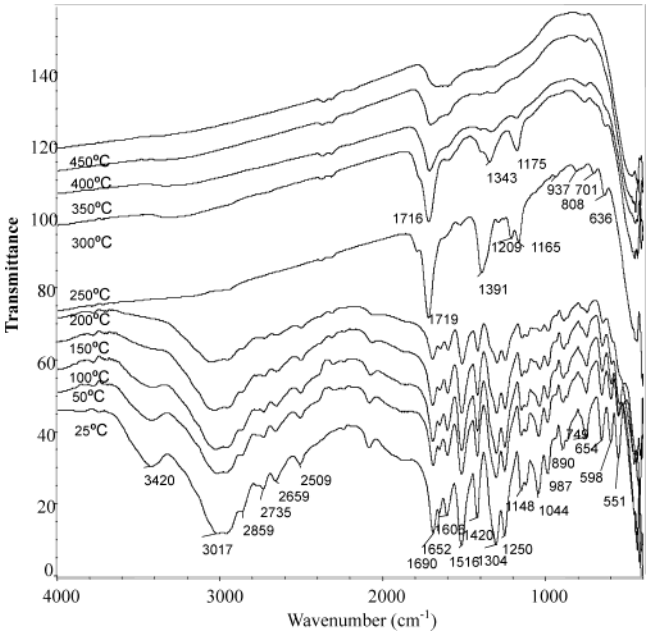

Figure 6. In situ FT-IR spectra for the thermal decomposition of L-Asp.

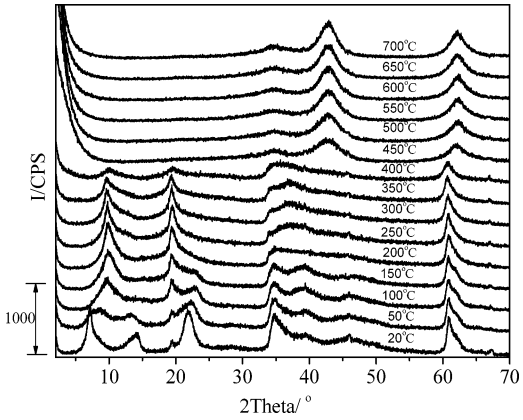

Figure 7. In situ XRD patterns for the thermal decomposition of L-Asp LDH in the temperature range 20∼700 °C.

water at about 3600 cm^{-1}, due to the formation of hydrogen bonding between interlayer water and guest anions as well as the hydroxide groups of the host layers.[41] The weak band at 2976 cm^{-1} corresponds to the asymmetric C−H stretching vibration. The strong absorptions at 1582 and 1397 cm^{-1} are characteristic of the asymmetric and symmetric stretching vibrations, respectively, of the carboxylic groups. The difference between the two frequencies (185 cm^{-1}) is close to the value expected for a bridging carboxyl group.[41] As is clear from the powder XRD patterns, Mg−Al−NO_3 LDH also coexists with L-Asp LDH, but no stretching vibration of nitrate (∼1385 cm^{-1})[23] is observed in the FT-IR, which is possibly because its absorption band is overlapped by the symmetric stretching vibration of the carboxyl group at 1397 cm^{-1}. The other absorption bands below 1000 cm^{-1} mostly arise from the mixed metal hydroxide layers.[42,43] The band centered at 665 cm^{-1} is assigned to M−O (M−O−M or O−M−O) stretching vibrations in the brucite-like sheet,[41] while the band at 452 cm^{-1} is assigned to layer lattice vibrations.[44,45] The band at 554 cm^{-1} is due to an M−O−H bending deformation vibration.[44,45]

On heating, the first change in the FT-IR spectra occurs between 25 and 150 °C. The band at 3450 cm^{-1} moves to higher frequency (3473 cm^{-1}) and its intensity decreases. This is probably related to the decrease in hydrogen bonding due to the loss of physically adsorbed water and interlayer water molecules. The asymmetric and symmetric stretching vibrations of the carboxyl group move to high frequency and low frequency, respectively. The difference between the two bands increases from 185 cm^{-1} at 25 °C to 206 cm^{-1} at 150 °C, indicating that the symmetry of the interaction between the carboxylate and hydroxyl layers has decreased with the loss of the interlayer water.[35,41] With the increase in temperature to 250 °C, the shoulder around 860 cm^{-1} originally present at 200 °C develops into a clearly visible band centered at 867 cm^{-1} and is indicative of a different kind of M−O stretching vibration. Additionally, the sharp lattice vibration band at 452 cm^{-1} splits into two bands, located at 460 and 438 cm^{-1}. This is most probably caused by the dehydroxylation of the layers that takes place at 250 °C. Remarkably, the asymmetric and symmetric stretching vibration bands of the carboxyl group shift to 1601

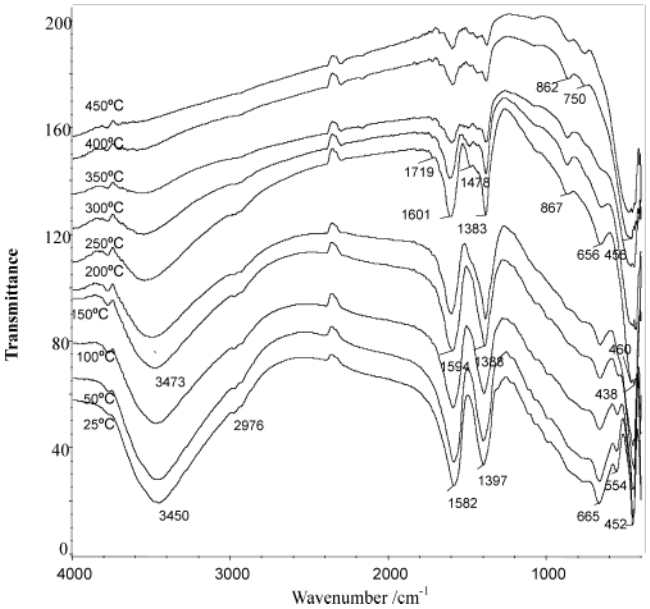

Figure 8. In situ FT-IR spectra for the thermal decomposition of L-Asp LDH.

and 1383 cm^{-1}, respectively. Furthermore, two new absorption bands at 1719 and 1478 cm^{-1} which correspond to butenedioate ions appear. Therefore, it can be concluded that the intercalated L-Asp has decomposed at 250 °C according to the reaction shown in Scheme 3. At this temperature, there are two kinds of carboxyl groups in the interlayer: aspartate and butenedioate. From 250 to 450 °C, the interlayer materials decompose and the layers dehydroxylate continuously, leading to a gradual decrease in the intensity of the absorption bands. At 400 °C, the bands at 862 and 750 cm^{-1} can be assigned to M−O vibrations in mixed oxide phase.

The solid-state ^{13}C NMR spectra of the as-synthesized L-Asp LDH and after heating at 220 °C for 24 h are shown in Figure 5, panels c and d, respectively. The spectrum of the as-synthesized material (Figure 5c) displays signals at 182.0 ppm (COO-), 181.3 ppm (COO-), 53.0 ppm (CHN), and 41.2 ppm (CH_2), consistent with the presence of L-Asp dianions. An additional peak at 170.3 ppm is probably due to surface-adsorbed carbonate. The spectrum is in good agreement with that of literature.[21] After heating (Figure 5d), a new resonance at 173.5 ppm [C(═O)−N in polysuccinimide] with two shoulders at 181 and 178.0 ppm (COO− in L-Asp) appears. In addition, CHN and CH_2 resonances in polysuccinimide are observed at 52.5 and 40.4 ppm, respectively. Furthermore, there are two new resonances observed at 161.3 ppm (COO− in butenedioate) and 135.4 ppm (C═C in butenedioate). The shoulder resonance at 164.7 ppm is due to the presence of imide [(C═O)−NR−(C═O)] in polysuccinimide.[21] The above NMR results suggest that L-Asp ions undergo the two reactions shown in Schemes 2 and 3 on calcination, whereas Whilton et al.[21] reported that only polymerization of L-Asp ions in the interlayer of LDH occurred on heat treatment.

Conclusions

L-Asp LDH was obtained by the method of coprecipitation. It is likely that guest anions are accommodated in the interlayer region as a monolayer with the two carboxylate groups electrostatically attracted to both upper and lower hydroxide layers, with a hydrogen-bonding network existing between water, the guest anions, and the host layers.

The thermolysis of L-Asp LDH is quite different from that of the pristine L-Asp studied as a reference sample and is characterized by three steps: the first from room temperature to 150 °C is attributed to the loss of both adsorbed and interlayer water, accompanied by the destruction of the hydrogen bonding network and a decrease in basal spacing; the second step (250−350 °C) involves the polymerization and deamination of L-Asp ions in the interlayer of LDH and dehydroxylation of the brucite-like layers; the third step in the temperature range of 350−450 °C corresponds to dehydroxylation of the brucite-like layers as well as further decomposition of interlayer materials. Solid-state ^{13}C NMR spectroscopy confirms that polymerization is the only reaction occurring when L-Asp is heated at 220 °C, while both polymerization and deamination of L-Asp ions in the interlayer of LDH take place after calcination at the same temperature. These observations may indicate that constriction of the L-Asp anions in the limited interlayer space of LDHs results in different chemical properties.

Acknowledgment. This project was supported by the National Natural Science Foundation of China (No. 90206004).

References and Notes

(1) Constantino, V. R. L.; Pinnavaia, T. J. *Catal. Lett.* **1994**, *23*, 361.
(2) Corma, A.; Fornés, V.; Rey, F.; Cervilla, A.; Llopis, E.; Ribera, A. *J. Catal.* **1995**, *152*, 237.
(3) Sels, B.; De Vos, D.; Buntinx, M.; Pierard, F.; Mesmaeker, K. D.; Jacobs, P. *Nature* **1999**, *400*, 855.
(4) Ukrainczyk, L.; Chibwe, M.; Pinnavaia, T. J.; Boyd, S. A. *Environ. Sci. Technol.* **1995**, *29*, 439.
(5) Ogawa, M.; Kuroda, K. *Chem. Rev.* **1995**, *95*, 399.
(6) Fogg, A. M.; Green, V. M.; Harvey, H. G.; O'Hare, D. *Adv. Mater.* **1999**, *11*, 1466.
(7) Fogg, A. M.; Dunn, J. S.; Shyu, S. G.; Cary, D. R.; O'Hare, D. *Chem. Mater.* **1998**, *10*, 351.
(8) Tagaya, H.; Sato, S.; Kuwahara, T.; Kadokawa, J.; Masa, K.; Chiba, K. *J. Mater. Chem.* **2002**, *4*, 1907.
(9) Newman, S. P.; Jones, W. *New J. Chem.* **1998**, *22*, 105.
(10) Khan, A. I.; O'Hare, D. *J. Mater. Chem.* **2002**, *12*, 3191.
(11) Carrado, K. A.; Kostapapas, A.; Suib, S. L. *Solid State Ionics* **1988**, *26*, 77.
(12) Hibino, T.; Yamashita, Y.; Kosuge, K.; Tsunashima, A. *Clays Clay Miner.* **1995**, *43*, 427.
(13) Hou, X. Q.; Bish, D. L.; Wang, S. L.; Johnston, C. T.; Kirkpatrick, R. J. *Am. Mineral.* **2003**, *88*, 167.
(14) Allmann, R. *Acta Crystallogr. B* **1968**, *24*, 972.
(15) Taylor, H. F. W. *Mineral. Mag.* **1973**, *39*, 377.
(16) Stecher, H.; Hermetter, A.; Faber, K. *Biotechnol. Tech.* **1998**, *12*, 257.
(17) Nijis, H.; Clearfield, A.; Vansant, E. F. *Microporous Mesoporous Mater.* **1998**, *23*, 97.
(18) Zhao, H. T.; Vance, G. F. *J. Chem. Soc., Dalton Trans.* **1997**, 1961.
(19) Moujahid, E. M.; Besse, J. P.; Leroux, F. *J. Mater. Chem.* **2002**, *12*, 3324.
(20) Ambrogi, V.; Fardella, G.; Grandolini, G.; Perioli, L. *Int. J. Pharm.* **2001**, *200*, 23.
(21) Whilton, N. T.; Vickers, P. J.; Mann, S. *J. Mater. Chem.* **1997**, *7*, 1623.
(22) Fudala, Á.; Pálinkó, I.; Kiricsi, I. *Inorg. Chem.* **1999**, *38*, 4653.
(23) Aisawa, S.; Takahashi, S.; Ogasawara, W.; Umetsu, Y.; Narita, E. *J. Solid State Chem.* **2001**, *162*, 52.
(24) Xu, Z. P.; Zeng, H. C. *J. Phy. Chem. B* **2000**, *104*, 10206.
(25) Pérez-Ramírez, J.; Mul, G.; Moulijn, J. A. *Vib. Spectrosc.* **2001**, *27*, 75.
(26) Kanezaki, E. *Solid State Ionics* **1998**, 106, 279.
(27) Loh, W. L.; Jaenicke, S.; Chuah, G. K.; Ang, H. G. *Talanta* **1998**, *45*, 739.
(28) Hou, Z. Y.; Yashima, T. *Catal. Lett.* **2003**, *89*, 193.
(29) Bookin, A. S.; Drits, V. *Clays Clay Miner.* **1993**, *41*, 551.
(30) Vaysse, C.; Guerlou-Demourgues, L.; Delmas, C. *Inorg. Chem.* **2002**, *41*, 6905.
(31) Bonnet, S.; Forano, C.; de Roy, A.; Besse, J. P.; Maillard, P.; Momenteau, M. *Chem. Mater.* **1996**, *8*, 1962.
(32) Millange, F.; Walton, R. I.; O'Hare, D. *J. Mater. Chem.* **2000**, *10*, 1713.
(33) Miyata, S. *Clays Clay Miner.* **1975**, *23*, 369.

(34) Wang X. C. *Biological Chemistry*; Tsinghua University Publishing House: 2001.
(35) Prevot, V.; Forano, C.; Besse, J. P. Abraham, F. *Inorg. Chem.* **1998**, *37*, 4293.
(36) Newman, S. P.; Cristina, T. D.; Coveney, V.; Jones, W. *Langmuir* **2002**, *18*, 2933.
(37) Challier, T.; Slade, R. C. T. *J. Mater. Chem.* **1994**, *4*, 367.
(38) Cavini, F.; Trifiro, F.; Vaccari, A. *Catal. Today* **1991**, *11*, 173.
(39) de Roy, A.; Forano, C.; Malki, K. E.; Besse, J. P. In *Expanded Clays and other Microporous Solids*; Occelli, M. L., Robson, H., Eds.; Van Nostrand: New York, 1992; Chapter 7.
(40) Rebours, B.; Jean-Baptiste, E. C.; Clause, O. *J. Am. Chem. Soc.* **1994**, *116*, 1707.
(41) Nakamoto, K. *Infrared and Raman Spectra of Inorganic and Coordination Compounds*, 5th ed.; Wiley & Sons: New York, 1997.
(42) Velu, S.; Sabde, D. P.; Shah, N.; Sivasanker, S. *Chem. Mater.* **1998**, *10*, 3451.
(43) del Arco, M.; Trujillano, R.; Rives, V. *J. Mater. Chem.* **1998**, *8*, 761.
(44) Kannan, S.; Swamy, C. S. *J. Mater. Sci.* **1997**, *32*, 1323.
(45) Li, L.; Ma, S.; Liu, X.; Yue, Y.; Hui, J.; Xu, R.; Bao, Y.; Rocha, J. *Chem. Mater.* **1996**, *8*, 204.